Silicon Carbide-Based Extreme Environment Hybrid Design Temperature Sensor Using Optical Pyrometry and Laser Interferometry

Nabeel A. Riza, *Fellow, IEEE*, and Mumtaz Sheikh

***Abstract*—To the best of the authors' knowledge, proposed and demonstrated is the first extreme environment temperature sensor using Blackbody (BB) radiation of a high-temperature material optical chip for coarse temperature measurement and classical Fabry-Perot (FP) laser interferometry via the same chip for fine temperature measurement. Such a hybrid design sensor can be used to accurately measure temperatures in excess of 750 °C such as needed for gas turbines in power plants and aircraft engines. The proposed sensor is designed and demonstrated using an all-Silicon Carbide (SiC) probe for temperatures from 795 °C to 1077 °C with an estimated average measurement resolution of 0.1 °C.**

***Index Terms*—Extreme temperature sensor, Fabry–Perot (FP) interferometer, pyrometer, silicon carbide (SiC).**

I. Introduction

THERMOCOUPLEs (TCs) have remained the preferred method for temperature sensing in the extreme environments of gas turbines where temperatures can reach 1600 °C. TCs tend to suffer from reliability and limited lifetime issues. Recently engineered are alternative temperature sensor designs using high-temperature optical materials such as advanced silica [1], sapphire [2], [3] and SiC [4]–[6]. Wired approaches to harsh environment temperature sensing, i.e., fiber-optic and electrical/TCs require subjecting the entire wire to the extreme conditions. Under these harsh conditions, fundamental wire material performances restrict sensor lifetimes. Optical pyrometry based on Planck's Blackbody (BB) radiation law has long been used to measure extreme temperatures [7]–[9]. One-color pyrometry uses a single radiation measurement in a limited spectral band and requires *a priori* knowledge of the specific emissivity of the target. Two-color pyrometry removes this emissivity limitation by using the ratio of irradiances at two different spectral bands. Recently, a hybrid fiber-freespace temperature sensor has been proposed and demonstrated using laser targeting of a silicon carbide (SiC) optical chip embedded inside a sintered SiC tube that forms an all-SiC probe [10]. This sensor used two laser interferometric methods, one for coarse and the other for fine temperature measurement inside a coarse measurement bin to deliver a direct measurement high resolution temperature sensor [11], [12]. Nevertheless, for industrial applications, it is highly desirable to have a fault-tolerant sensing system with built-in redundancy. Hence, this paper shows how an all-SiC probe can use two-color pyrometry and FP laser interferometry to realize an alternate signal processing chain high resolution extreme environment temperature sensor.

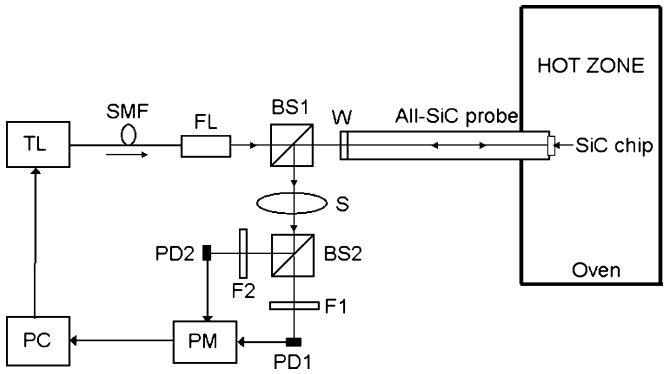

Fig. 1. Proposed high-resolution extreme environment temperature sensor. SMF: single-mode fiber; PC: personal computer.

II. Proposed SiC-Based Hybrid Design Temperature Sensor

Fig. 1 shows the proposed sensor design. For coarse temperature measurement, the SiC chip is used as a BB radiator in a two-color pyrometer configuration. The spectral radiance of an ideal BB radiator is given by Planck's law

$$I(\lambda, T) = \frac{2hc^2}{\lambda^5} \frac{1}{e^{\frac{hc}{\lambda kT}} - 1}. \quad (1)$$

λ is the emitted radiation wavelength, T is the BB temperature in Kelvins, h is the Planck's constant, c is the speed of light, and k is the Boltzmann's constant. In addition to radiation emitted from the SiC chip, background radiation caused by stray furnace light or another heat source is also detected by the photodetectors [7]. One can assume that the SiC chip and the background radiation source are at the same temperature as SiC has a high (e.g., 120 W/m.K) thermal conductivity. Hence, using (1) under the Wein approximation (i.e., $\mathrm{hc} \gg \lambda \mathrm{kT}$), the ratio of output

Manuscript received June 07, 2009; revised July 29, 2009; accepted August 15, 2009. Current version published December 28, 2009. The associate editor coordinating the review of this paper and approving it for publication Prof. Eh Yang.

The authors are with the Photonic Information Processing Systems Laboratory, CREOL, The College of Optics and Photonics, University of Central Florida, Orlando, FL 32816-2700 USA (e-mail: riza@creol.ucf.edu; msheikh@creol.ucf.edu).

Color versions of one or more of the figures in this paper are available online at http://ieeexplore.ieee.org.

Digital Object Identifier 10.1109/JSEN.2009.2031425

detected BB radiation powers at the two wavelengths of interest λ_1 and λ_2 is given by [8]

$$R = \frac{P_{\lambda_1}}{P_{\lambda_2}} = A_S \left(\frac{\lambda_2}{\lambda_1}\right)^5 \frac{\varepsilon(\lambda_1, T) + a(\lambda_1, T)}{\varepsilon(\lambda_2, T) + a(\lambda_2, T)} \times \exp\left[-C_2\left(\frac{1}{\lambda_1} - \frac{1}{\lambda_2}\right)\frac{1}{T}\right]. \quad (2)$$

A_S is a sensor-specific constant that takes into account spectral transmittance of the optical sensor system, spectral response and the bandwidth of the optical filters F1 and F2, and the responsivity of the photodetectors PD1 and PD2. $\varepsilon(\lambda, T)$ is the specific emissivity of SiC, $a(\lambda, T)$ is the product of the emissivity of the background radiation source and its transmission percentage through the system and $C_2 = \mathrm{hc/k}$. The emissivities also have a weak dependence on λ provided there are no sharp emission lines near either of the two working wavelengths. If the two wavelengths are selected close to each other, then the effect of ε on the ratio is minimal and (2) can be written as [8]

$$\ln R = \alpha + \frac{\beta}{T}. \quad (3)$$

α and β are constants that can be determined by sensor calibration. Once α and β are determined, a coarse value of temperature can be determined by measuring the ratio R and finding the corresponding value of T from the calibrated R against T curve. For fine temperature measurement, the SiC chip is used as a FP etalon with reflectance given by

$$R_{FP} = \frac{R_1 + R_2 + 2\sqrt{R_1 R_2}\cos\varphi}{1 + R_1 R_2 + 2\sqrt{R_1 R_2}\cos\varphi}. \quad (4)$$

R_1 and R_2 are the classic Fresnel Power coefficients for the SiC-air interface given by $R_1 = R_2 = [(1-n)/(1+n)]^2$ and $\varphi = (4\pi/\lambda)\ n(T)t(T)$. At temperature T, $n(T)$ is the chip refractive index at laser wavelength λ and $t(T)$ is the chip thickness. The reflected laser power $P(\lambda, T)$ is proportional to R_{FP} and has a sinusoidal behavior with φ. The change in P due to change in λ can be written as:

$$\frac{dP}{d\lambda} = \frac{dP}{d\varphi}\frac{d\varphi}{d\lambda} = -\frac{4\pi}{\lambda^2} n(T)t(T)\frac{dP}{d\varphi}. \quad (5)$$

Equation (5) implies that if $dP/d\lambda$ is positive, i.e., the reflected power increases with an increase in wavelength, then $dP/d\varphi$ would be negative and *vice versa*. The normalized SiC chip reflected laser light power P_{norm} is given by

$$P_{\mathrm{norm}} = \frac{P - P_{\min}}{P_{\max} - P_{\min}}. \quad (6)$$

$P_{\max}$ and $P_{\min}$ are the localized maximum and minimum power values. To determine a given T, first the two-color pyrometer is used to find a coarse value of temperature within one 2π cycle (alternatively referred to as a coarse bin) of the P_{norm} against φ curve. Next, within that P_{norm} cycle (or coarse bin), the normalized reflected power is measured at a fixed laser wavelength $\lambda = \lambda_L$ along with the sign of the change in detected power with change in λ. Specifically, Fig. 2(a) shows that at a given temperature, the measured optical power reading P_m within a coarse bin indicates two temperatures values of T_1 and T_2. Given that only one of them is the true temperature, there is a two state ambiguity problem within a coarse bin. Fig. 2(b) shows via a graphical display as to how the slope or $dP/d\lambda$ sign measurement is used for selecting either T_1 or T_2 as the true unambiguous temperature for the proposed sensor. The exact value of T can then be found from a previously calibrated P_{norm} against T curve at λ_L [11].

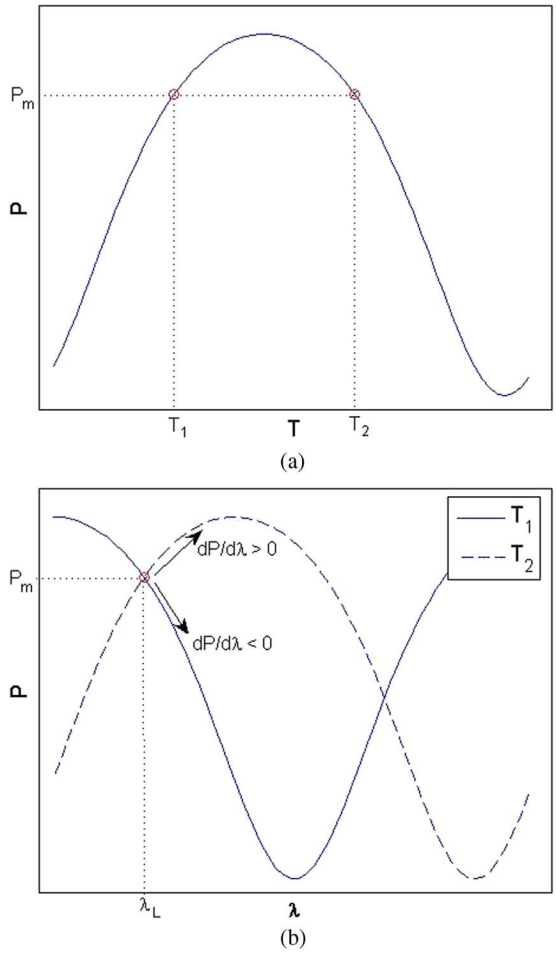

Fig. 2. (a) A graphical display showing that at a given temperature, the measured optical power reading P_m within a coarse bin indicates two temperatures values of T_1 and T_2 and only one of them is the true temperature. (b) A graphical display of the slope or $dP/d\lambda$ sign measurement working principle for selecting either T_1 or T_2 as the unambiguous temperature for the proposed sensor.

III. Experimental Results and Discussion

The Fig. 1 proof-of-concept experiment is setup in the laboratory with SiC chip $t = 389\ \mu\mathrm{m}$. The probe is inserted into an oven. BB radiation from the SiC chip and the background passes through an optical window W. After deflection from the beamsplitter BS1, radiation is captured using a 10 cm focal length spherical lens S and directed towards another beam splitter BS2 and then towards two 3 mm diameter Newport photodetectors PD1 and PD2. Optical filters F1 and F2 are Newport laser line models 10LF30-1550 and 10LF30-1300 having center wavelengths λ_1 and λ_2 of 1550 ± 7 nm and 1300 ± 7 nm, respectively. The filters have a FWHM bandwidth of 30 ± 7 nm. An

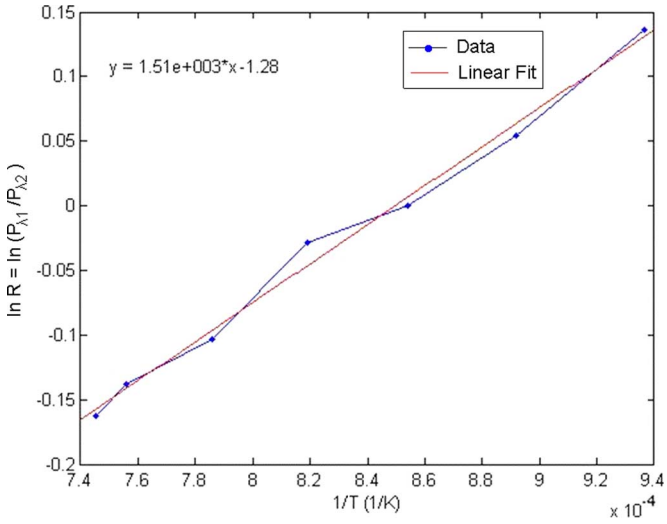

Fig. 3. Experimentally measured ln R versus $1/T$ curve and the corresponding line of best fit.

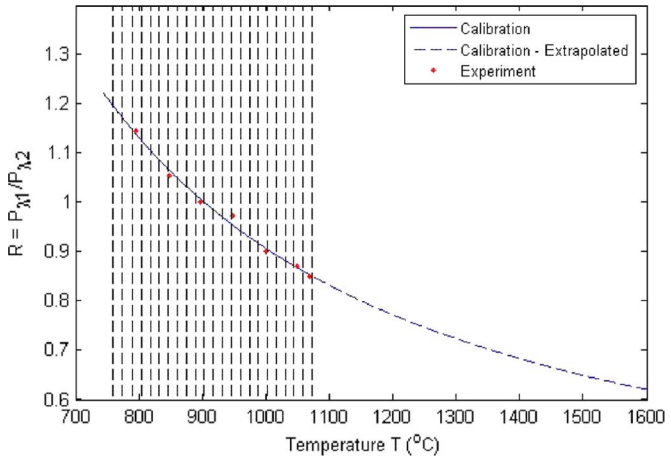

Fig. 4. R versus T calibration curve using α and β derived from curve fitting along with experimentally measured temperatures using optical pyrometry.

R-type TC is used to measure the oven reference T. For laser interferometry is used a tunable laser TL Santec TSL-210 with a wavelength tuning range of 1520–1600 nm and peak power of 10 mW. The fiber lens (FL) has a working distance of 60 cm and $1/e^2$ minimum beam waist diameter of 0.53 mm formed at the SiC chip. Light from the FL strikes the SiC chip at normal incidence and in the return path, is deflected from BS1 and BS2 and is focused onto PD1. TL is set to $\lambda_L = 1550$ nm.

The oven is set at ~ 50 °C intervals starting at $T = 795$ °C. Optical power meter PM readings are taken with TL on and with TL off. Fig. 3 shows how ln R varies with 1/T and a linear line of best fit is found in accordance with (3) that, in turn, gives $\alpha = -1.282$ and $\beta = 1509$. Note that if the Wein approximation is not used and instead the exact Planck's BB radiation formula is used [7], $\alpha = -1.285$ and $\beta = 1512$. Given that the proposed sensor uses pyrometry for coarse temperature measurement, using the Wein approximation is justified and leads to simpler signal processing. Assuming that the center wavelengths of the laser line filters are 1543 and 1307 nm within the manufacturer tolerance limits, the theoretical value of β from (2) and (3) is found to be 1684. Note that the linear model in (3) is developed under the assumption that $A_S(\lambda)\,\varepsilon(\lambda, T)$ and $a(\lambda, T)$ in (2) are all independent of λ. In practice, these are all weakly dependent on λ and this can cause deviation of β from the theoretical value. Fig. 4 shows the R against T calibration curve extrapolated to 1600 °C based on the linear fit from Fig. 3. A coarse value of the temperature can simply be found by measuring R and finding the corresponding T value from Fig. 4. Note that this calibration curve is only valid for the Fig. 1 specific experimental arrangement, i.e., heating via the deployed oven with its specific background radiation in the output detected power. For a different heating environment, the sensor would have to be recalibrated to take into account the differing levels of background radiation. Note that for the sensor to be used in all environments, sensor calibration requires the background radiation to be blocked at the λ_1 and λ_2 wavelengths of interest. This can readily be achieved by using a capped front-end all-SiC probe design that would prevent optical background radiation from entering the light paths to the detectors. Such a design would also prevent the SiC chip from coming into direct contact with contaminants such as water vapor present in the extreme turbine environments, thus preventing elevated temperature oxidation of the SiC sensor chip. In addition, the all-SiC probe cavity is closed using the optical window (W) and a partial vacuum (25 in Hg) is maintained inside the probe. Ideally, a vacuum or hermetic sealed probe would remove any possibility of the SiC chip and SiC probe internal cavity from oxidizing.

The resolution of the pyrometer depends on the smallest change in optical power that can be detected by PD1 and PD2 (with laser off) based on the noise present in the system. The change in T due to a change in R can be written by differentiating (3) with respect to R and is given as

$$\Delta T = \frac{-\beta}{R(\ln R - \alpha)^2}\Delta R. \tag{7}$$

Using (2) and taking partial derivatives of R with respect to $P_{\lambda 1}$ and $P_{\lambda 2}$, ΔR can be further written in terms of change in detected powers $P_{\lambda 1}$ and $P_{\lambda 2}$ as

$$\Delta R = \frac{\Delta P_{\lambda_1} - R \cdot \Delta P_{\lambda_2}}{P_{\lambda_2}}. \tag{8}$$

The smallest change in radiation power that can be detected based on the noise in the present system is $\Delta P_{\lambda 1} = \Delta P_{\lambda 2} = 0.01\ \mu$W. At $T = 795$ °C, $R = 1.14$ and $P_{\lambda 2} = 0.16\ \mu$W, while at $T = 1077$ °C, $R = 0.85$ and $P_{\lambda 2} = 0.80\ \mu$W. Based on these numbers and using (7) and (8), the resolution of the pyrometer is estimated to vary between 5.8 °C at 795 °C to 2.7 °C at 1077 °C. Note that this resolution is sufficient to identify the correct 2π cycle for fine temperature sensing as each cycle is approximately 15 °C. Recall that FP laser interferometry (used for fine temperature sensing) can only be used to determine temperature unambiguously within one 2π cycle of the P_{norm} against φ curve. These 2π cycles are shown marked on Fig. 4 as vertical dashed lines indicating how a specific measured value of R can be used to determine in which 2π cycle the temperature being measured belongs. The experimentally measured R values are also shown in Fig. 4 that are used to identify the 2π cycle to which the temperature belongs. Once the correct 2π cycle is

TABLE I
COMPARATIVE MEASUREMENTS OF T USING TC, TWO COLOR OPTICAL PYROMETRY, AND THE HYBRID SENSOR

TC T (^{O}C)	PYROMETER ONLY T (^{O}C)	SENSOR MEASURED T (^{O}C)
795.0	791.0	798.5
848.0	856.0	850.5
897.7	904.0	898.5
946.5	930.5	944.0
999.5	1006.5	1002.5
1049.0	1045.5	1051.5
1077.0	1069.0	1077.0

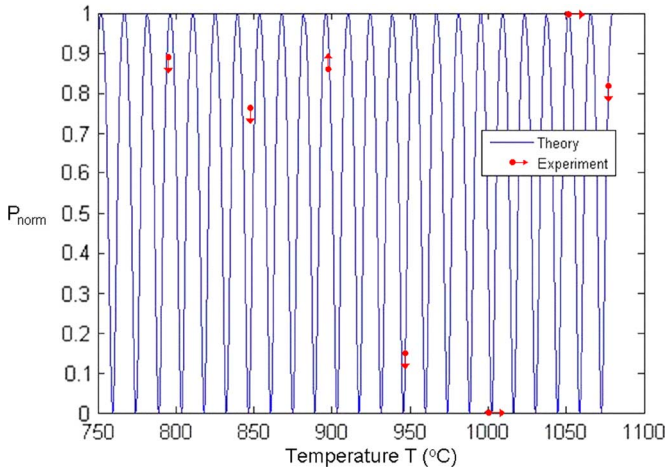

Fig. 5. Computed and experimentally measured $P_{\rm norm}$ against T curve for fine temperature sensing.

identified, then with the TL on, the PD1 power is measured that includes both laser reflected power as well as the BB radiation power. The laser reflected power, however, is much greater than the radiation power and is normalized by simply tuning the wavelength to find localized power maxima and minima values and using (6) to find $P_{\rm norm}$. Also, by tuning the wavelength, the direction of the change in power with wavelength is determined (shown by arrows in Fig. 5) in accordance with (5) to distinguish between the two halves of the 2π cycle. These results are shown in Fig. 5 along with the expected theoretical curve for the normalized laser reflected power with temperature based on previous experiments [11], [12]. The T resolution for this laser technique (and sensor) is also determined by the smallest change in optical power detected by PD1 (with laser on) based on the noise in the system. This smallest change is measured to be $\Delta P = 0.001$ mW with a $P_{\rm max} - P_{\rm min} = 0.079$ mW for an average 7.5 °C change in T. These numbers give an estimated average 0.1 °C resolution for the sensor. Table I shows comparative measurements of T using the two color (TC) optical pyrometry, and the proposed hybrid sensor. The results show a sensor measured maximum T difference of 0.44% compared to the TC readings.

Note that using the proposed hybrid sensing approach, an error in temperature measurement could arise if the temperature being measured lies close to the boundary of the calibrated coarse temperature bins defined by the 2π temperature cyclic data (e.g., Fig. 5) via single wavelength laser-based FP interferometry of the SiC chip. Thus a slight experimental error in the coarse temperature measurement could result in identification of the wrong 2π cycle or coarse temperature bin leading to a large error in the signal processing-based measured temperature. Another issue related to the proposed signal processing is the possibility of reduced fine temperature measurement sensitivity (or resolution) controlled by the slope of the $P_{\rm norm}$ versus T curve or dP/dT (see Fig. 5) close to the maxima or minima of this cyclic curve. Specifically, the slope of the curve approaches zero close to these max/min temperature points resulting in decreased sensor temperature measurement resolution. Both these mentioned signal processing limitations can be circumvented by calibrating the optical probe at two slightly different laser wavelengths λ_1 and λ_2 instead of one specific wavelength such that there is a $\pi/2$ to π phase difference between the two calibration curves (see Fig. 6). This process would result in two sets of coarse bin boundaries, one each for λ_1 and λ_2, relatively displaced from each other so that no temperature value could simultaneously lie close to the coarse bin boundary for both λ_1 and λ_2.

Note that if the coarse temperature measurement gives a temperature value that lies near the boundary for λ_1, then λ_2 could be used for fine temperature measurement to give an accurate temperature value and vice versa. At the same time, it would also ensure that any given temperature value would fall in the highly sensitive region of the $P_{\rm norm}$ versus T calibration curve for at least one of λ_1 and λ_2 power readings, thus resulting in high-resolution temperature measurement for all temperatures measured by the sensor. Note that for the coarse temperature boundary indecision problem, the ideal phase difference between the two calibration curves is π radians (see Fig. 6(a)) as it gives the highest discrimination between the two sets of laser power cycle boundaries. In the worst-case scenario shown by a square marker in Fig. 6(a), the measured temperature is at least $\pi/2$ radians away from a cycle boundary that for the present experiment would amount to $\sim$ 4 °C (see Fig. 5 as one cycle is $\sim$ 16 °C). Note that for optimal sensor temperature sensitivity, the ideal value for the calibration cyclic power two wavelength phase difference is $\pi/2$. This is because if the temperature value falls on the maxima or minima for λ_1, it also falls on the most sensitive part of the curve for λ_2 [see Fig. 6(b)] and *vice versa*. Example of these temperatures with the curve slopes of zero are indicated by diamonds on the $P_{\rm norm}$ versus T curves in Fig. 6(b) and indeed show that their corresponding second wavelength power values (shown as triangles) fall on the highly sensitive parts of their second wavelength curve. The temperatures with the least sensitivity in this two-wavelength calibration scenario, $(\pi - \pi/2)/2 = \pi/4$ radians away from the maximas or minimas of both curves, are indicated by circles on the

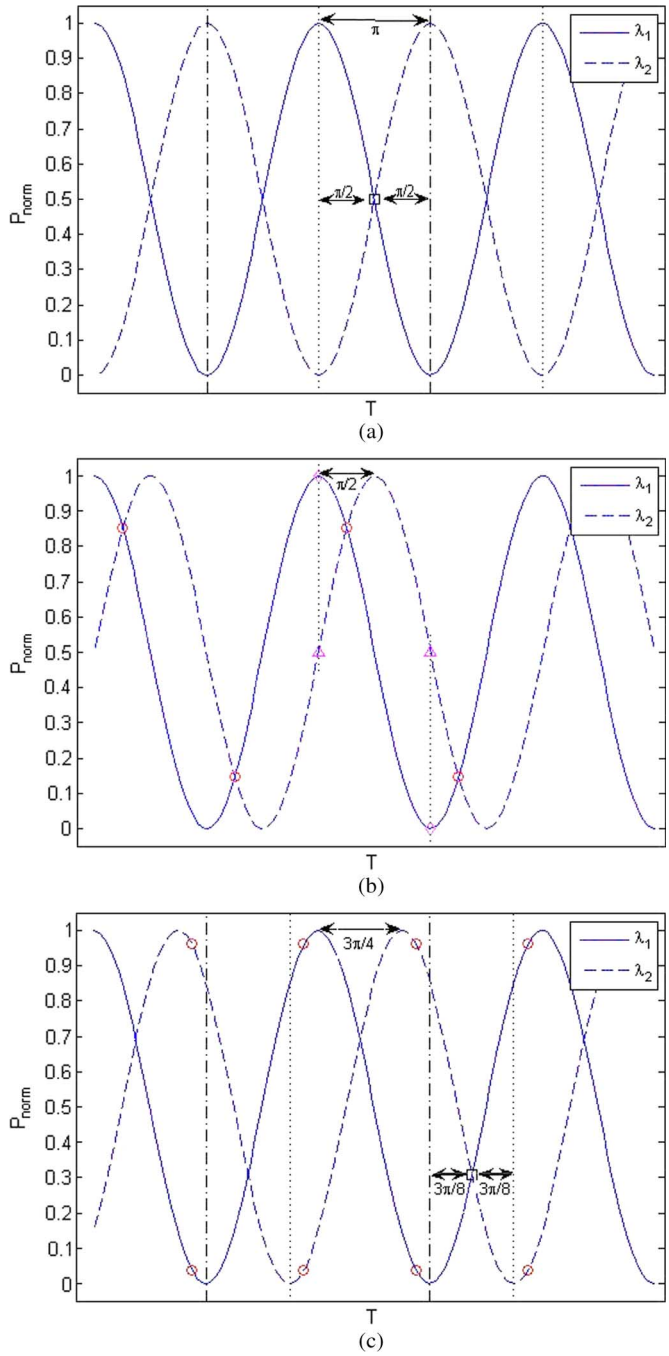

Fig. 6. Sensor signal processing calibration curves at two wavelengths λ_1 and λ_2 with relative curve phase differences of (a) π, (b) $\pi/2$, and (c) $3\pi/4$. Vertical lines in (a) and (c) denote the 2π cycle boundaries at each wavelength that determine sets of coarse bins for sensor calibration.

$P_{\rm norm}$ versus T curve in Fig. 6(b) and still fall on highly sensitive parts of the curve. For the present experiment, this least sensitivity sensor temperature resolution would be 0.09 °C as found by numerically by finding the slope of the curve in Fig. 5 with a 0.001 mW optical power change. As shown in Fig. 6(c), calibration curves with relative phase shift value between π and $\pi/2$ would equally account for both coarse bin boundary and sensor resolution issues, although the specific choice of phase difference would depend on experimental considerations such as the probability of error and the resolution of the coarse measurement. For example, using a phase difference of $3\pi/4$ [see Fig. 6(c)], any measured temperature is at least $3\pi/8$ radians away from a coarse bin boundary (shown as a square on the figure), or equivalently $\sim$ 3 °C for the reported experiment. In this case, the temperatures with the least sensitivity [again shown by circles on Fig. 6(c)] are $(\pi - 3\pi/4)/2 = \pi/8$ radians away from the maximas or minimas of both curves. Although the sensitivity is reduced from the case of Fig. 6(b), it is still comparable to the average value for the sensor. Specifically, for the present experiment this least sensitivity temperature resolution value is found from Fig. 5 to be 0.16 °C.

IV. Conclusion

In conclusion, SiC-based two-color pyrometry is combined with FP laser interferometry to deliver a new signal processing method for an all-SiC probe high resolution extreme temperature sensor enabling fault-tolerant dual-mode temperature sensing. The proposed sensor is ideally expected to work below the $\sim$ 2700 °C sublimation temperature of SiC. Note that the all-SiC probe used in this experiment has already been subjected to extensive structural, thermal and chemical robustness tests in the laboratory [13], [14]. In addition, it has also been recently tested in a Siemens industrial combustor rig over an extended period of time for feasibility and reliability checks in an extreme combustor environment [15]. Future work involves optimizing the all-SiC probe design for ideal calibration that can lead to use in all sensing conditions.

Acknowledgment

The authors thank Nuonics, Inc. for the all-SiC probe and DOE for program support. In addition, the authors thank Dr. F. Perez of Nuonics, Inc., for his original contributions to the sensor design.

References

[1] D. Grobnic, C. W. Smelser, S. J. Mihailov, and R. B. Walker, "Isothermal behavior of fiber Bragg gratings made with ultrafast radiation at tempertaures above 1000 °C," in *Proc. Eur. Conf. Opt. Comm. (ECOC)*, Stockholm, Sweden, 2004, vol. 2, pp. 130–131.

[2] D. Grobnic, S. J. Mihailov, C. W. Smelser, and H. Ding, " Ultra high temperature FBG sensor made in Sapphire fiber using femtosecond laser radiation," in *Proc. ECOC.*, Stockholm, Sweden, 2004, vol. 2, pp. 128–129.

[3] Y. Zhang, G. R. Pickrell, B. Qi, A. S.-Jazi, and A. Wang, "Single-crystal sapphire-based optical high temperature sensor for harsh environments," *Opt. Eng.*, vol. 43, pp. 157–164, 2004.

[4] G. Beheim, "Fibre-optic thermometer using semiconductor-etalon sensor," *Electron. Lett.*, vol. 22, pp. 238–239, 1986.

[5] L. Cheng, A. J. Steckl, and J. Scofield, "SiC thin film Fabry-Perot interferometer for fiber-optic temperature sensor," *IEEE Trans. Electron Devices*, vol. 50, pp. 2159–2164, 2003.

[6] N. A. Riza, M. A. Arain, and F. Perez, "Harsh environments minimally invasive optical sensor using freespace targeted single crystal silicon carbide," *IEEE Sensors J.*, vol. 6, pp. 672–685, 2006.

[7] Y. A. Levendis, K. R. Estrada, and H. C. Hottel, "Development of multicolor pyrometers to monitor the transient response of burning carbonaceous particles," *Rev. Sci. Instrum.*, vol. 63, pp. 3608–3622, 1992.

[8] U. Anselmi-Tamburini, G. Campari, G. Spinolo, and P. Lupotto, "A two-color spatial-scanning pyrometer for the determination of temperature profiles in combustion synthesis reactions," *Rev. Sci. Instrum.*, vol. 66, pp. 5006–5014, 1995.

[9] D. Ng and G. Fralick, "Use of a multiwavelength pyrometer in several elevated temperature aerospace applications," *Rev. Sci. Instrum.*, vol. 72, pp. 1522–1530, 2001.

[10] N. A. Riza, M. Sheikh, and F. Perez, "Design and fabrication of an extreme temperature sensing optical probe using silicon carbide technologies," in *Proc. IEEE Sensors Conf.*, 2007, pp. 660–663, I-4244-1262-5/07.

[11] N. A. Riza and M. Sheikh, "Silicon-carbide-based extreme environment temperature sensor using wavelength-tuned signal processing," *Opt. Lett.*, vol. 33, pp. 1129–1131, 2008.
[12] M. Sheikh and N. A. Riza, "Direct measurement high resolution wide range extreme temperature optical sensor using an all-silicon carbide probe," *Opt. Lett.*, vol. 34, pp. 1402–1404, 2009.
[13] M. Sheikh and N. A. Riza, "Experimental studies of an all-silicon carbide hybrid wireless-wired optics temperature sensor for extreme environments in turbines," in *Proc. SPIE Optical Sensing IV Conf.*, Apr. 2008, vol. 7003, p. 70030C.
[14] N. A. Riza and M. Sheikh, "All-silicon carbide hybrid wireless-wired optics temperature sensor: Turbine tests and distributed fiber sensor network design," presented at the SPIE Photonics Europe, Conf. n Optical Sensors, Prague, Czech Republic, Apr. 21, 2009, paper No. 24, Vol. 7356.
[15] N. A. Riza, M. Sheikh, and F. Perez, "Hybrid wireless-wired optical sensor for extreme temperature measurement in next generation energy efficient gas turbines," *ASME J. Eng. Gas Turbines Power*, vol. 132, no. 1, Jan. 2010.

Nabeel A. Riza (M'85–SM'94–F'07) received the Ph.D. degree in electrical engineering from the California Institute of Technology, Pasadena, 1989.

After completing the Ph.D. degree in 1989, he joined the General Electric Corporate Research and Development Center. In 1995, he joined CREOL, The College of Optics and Photonics, University of Central Florida (UCF), where he is a Professor of Optics.

Dr. Riza received the 2001 International Commission of Optics (ICO) Prize. He is a Fellow of the Optical Society of America (OSA) and the International Society for Optical Engineering (SPIE).

Mumtaz Sheikh received the B.Sc. (Hons) degree in Computer Science from Lahore University of Management Sciences (LUMS), Lahore, Pakistan. He is currently working towards the Ph.D. degree at the University of Central Florida (UCF), Orlando.

Mr. Sheikh is a recipient of the 2009 SPIE Scholarship.